Beta decay of Rb^{86*}

Richard H. Thompson and Karl J. Casper

Western Reserve University, Cleveland, Ohio

22126

Abstract: The beta decay of Rb^{86} has been measured using lithium drifted surface barrier silicon detectors. Corrections to the spectrum have been made using the measured response function of the detectors. The inner branch has an allowed spectral shape and an endpoint energy of 677 ± 5 keV, and the outer branch has a first forbidden unique spectral shape and an endpoint energy of 1753 ± 4.5 keV.

author

UNPUBLISHED PRELIMINARY DATA

1. Introduction

For many years the standard instruments for the measurement of the endpoint energy of a continuous beta-ray spectrum have been absorbers, magnetic spectrometers, and scintillation counters. By virtue of its superior resolution, the magnetic spectrometer has usually provided the most accurate measurement of the endpoint energy. Where the nuclide has a short half-life, scintillation counters with organic phosphors have generally been more effective.

Quite often, the beta decay contains more than one beta ray branch with each transition having a different endpoint energy. In these cases, either spectrum stripping or coincidence techniques may be used to determine

---

*Research supported in part by a grant from the National Aeronautics and Space Administration.

the endpoint energies of the inner branches. In the former, the shape of the beta-ray spectrum having the highest endpoint energy is determined so that the Fermi-Kurie plot is linearized. By extrapolation, this spectrum is then subtracted from the total measured spectrum. The branch having the next lowest endpoint energy is then analyzed in a similar manner, and this process is continued until all beta components have been determined.

In coincidence measurements, a gamma ray counter imposes the requirement that the beta ray be in coincidence with a gamma ray transition in the daughter nucleus. If the chance coincidence counting rate is small relative to the real coincidence counting rate, the inner beta ray spectrum will then be observed with few random counts from higher energy beta rays. The real coincidence counting rate N_R is given by

$$N_R = N\Omega_1 \Omega_2 e_1 e_2$$

where N is the decay rate of the source, Ω_1 Ω_2 refer to the solid angles subtended by the two detectors, and e_1 e_2 refer to the efficiencies of the detectors. While it would seem that one could increase the real coincidence rate simply by increasing the source intensity, the ratio of the chance to real coincidence rate is given in first order by

$$N_c/N_R = 2tN$$

where 2t is the resolving time of the coincidence circuit. This ratio should be kept as low as possible since a high value of this first order term is a strong indication that higher order chance coincidence terms will also contribute to the counting rate.[1] Therefore, in order to increase

the real coincidences, the solid angles must be improved. In magnetic spectrometers, it is possible to increase the solid angle, but this is generally at the expense of momentum resolution. Scintillation counters can approach a 4π geometry for each detector, but their poor energy resolution makes it difficult to calibrate the counters and to collect useful information about the shape of the beta-ray spectrum.

Solid state particle detectors with large depletion depths and negligible entrance windows provide a new measuring instrument, combining the advantages of energy resolution comparable to that of magnetic spectrometers with the experimental simplicity of scintillation counters. Thus, for the beta ray energies of this experiment, the solid state detector resolution corresponds to a momentum resolution of 1% to 2%. Moreover, in contrast to the magnetic spectrometer where only a small portion of the spectrum is measured at one time, the solid state detector can be used with a multichannel analyzer so that data may be rapidly accumulated. In coincidence experiments, the solid state detectors can also be arranged so that large solid angles are subtended.

Previous experimental results[2-7] on the beta decay of Rb^{86} have been obtained with magnetic spectrometers and scintillation counters. These results are shown in table 1; the agreement of the values of the endpoint energies of the inner and outer branches of the beta decay is not particularly good among these experiments.

Since the 676 keV beta-ray transition is one of the first-forbidden decays which exhibit a strong beta-gamma directional correlation, it should yield significant information about the matrix elements of the beta decay.

The correct determination of these matrix elements depends upon both the endpoint energy and the shape of the beta-ray spectrum. The primary purpose of the experiments described here is the determination of these last two quantities.

2. Beta-ray measurements with solid state detectors

Lithium drifted surface barrier silicon detectors were fabricated using relatively standard methods.[8] A number of such detectors having areas ranging from 0.8 cm^2 to 1.5 cm^2 and depletion depths ranging from 3 mm to 6 mm were used in the measurements. These detectors have the advantage of negligible window thickness and were constructed so that their entire volume was sensitive. They were mounted in Lucite holders of 2 cm inside diameter to eliminate scattering from high Z material near the detector. The resolutions of these detectors at room temperature ranged between 18 and 35 keV for the 975 keV internal conversion line of Bi^{207}. No attempt was made to improve this figure by cooling the detector.

The beta-ray spectrum that one obtains with a silicon particle detector is distorted from the true spectrum for three main reasons:

1. the detector has a finite energy resolution;
2. there is incomplete energy loss by the incident particles, as a result of back scattering from the face of the crystal and of incident electrons scattering out the sides of the crystal;
3. as a result of trapping, recombination, and low electric field regions near the edge of the detector, charge collection is

not complete and becomes smaller as the energy of the incident particle increases.

The effect of these distortions on the spectrum can be determined if the response of the detector to a monoenergetic electron is known over the energy range of interest. In this experiment, the response function was initially determined with a 180^{o} beta-ray spectrometer. The beta decay of P^{32} provided a source of electrons whose energies ranged to 1.7 MeV. The momentum resolution of the spectrometer was set at 2% and measurements were made at 200 keV intervals up to 1.6 MeV. A typical spectrum of one of these measurements is shown in fig. 2. Internal scattering of electrons from the baffles has introduced some distortion in the spectrum; however, the general shape is readily evident. In the calculations, the assumption was made that the response function has the simple shape shown in fig. 3.

The most important result of this spectrometer measurement is the variation of the response function with energy. An appropriate parameter which specifies this variation is the ratio of the number of counts under the peak to the total area; i.e., the relative number of counts whose energy is measured correctly. This ratio has a strong energy dependence as is shown in fig. 4 which shows the characteristic response of a 6 mm thick, 1.2 cm diameter detector. It should be emphasized that different detectors have response functions which maintain the shape shown in fig. 3, but differ considerably in the ratio of peak to total area. This result means that it is necessary to measure the response function of every detector before bata ray measurements can be performed with it.

The procedure for developing the true beta ray spectrum from the measured one follows the method of Freedman, Novey, Porter and Wagner.[9]

Their basic equation for determining the correct beta ray spectrum is

$$N_m(W) = \int_o^{W_o} N_t(W')\ L(W,W')\ dW' \qquad (1)$$

where $N_m(W)$ is the measured spectrum, $N_t(W)$ is the true (undistorted) wpectrum, $L(W,W')$ is the response function and W_o is the maximum beta ray energy. As a first approximation, the measured spectrum N_m is substituted for N_t in equation 1 and the integration performed to give N_m'. The next approximation to the true spectrum is obtained by forming the sum

$$N_t' = 2N_m - N_m'$$

which is then substituted into the integral. The process is repeated until N_m as obtained from equation 1 agrees closely with the measured spectrum.

Before performing this iteration process, it was found convenient to fit the measured spectrum with a smooth curve using Tchebycheff polynomials.[10] This avoids the magnification of statistical fluctuations into large peaks in the interation process. After the interation is completed, the original data points were multiplied by a factor obtained from a comparison of N_t and N_m.

3. Experimental apparatus and procedure

The sources of Rb^{86} used in this experiment were obtained from Oak Ridge National Laboratory in the form of RbCl in Hcl solution. Fresh sources were used to minimize the effect of minute impurities such as Co^{60}. A 60 μ aluminized Mylar foil was mounted on a 1.2 cm diameter,

0.5 mm thick aluminum ring. The source in solution was deposited on this foil and evaporated to dryness. Sources of Tl^{204} and P^{32} were also prepared in this manner.

The first measurements were made on the well-known spectra of P^{32} and Tl^{204}. These were very appropriate for this experiment since P^{32} is an allowed beta decay with an endpoint energy of 1.7 MeV very near to that of Rb^{86}, and Tl^{204} has a first-forbidden unique shape with an endpoint energy of 764 keV which is only slightly greater than that of the inner branch of Rb^{86}. Using the measured response function to correct the spectra, the resulting Fermi-Kurie plots were nonlinear. This effect was ascribed to the distortion of the response curve by internal baffle scattering of electrons in the magnetic spectrometer. That is, beta rays whose energy is outside the range that is being selected by the spectrometer can be scattered onto the detector and counted. To compensate for this effect, the response function in each case was adjusted slightly until the P^{32} and Tl^{204} spectra gave linear Fermi-Kurie plots

As a check on the accuracy of the analysis, the endpoint energies of the P^{32} and Tl^{204} decays were evaluated and found to be 1708 $\pm$ 5 keV and 761 $\pm$ 4 keV, respectively. Both of these values are in good agreement with other experimental results on these decays, thereby supporting the accuracy of the determination of endpoint energies in this experiment.

Four different detectors were used to measure the outer branch of the Rb^{86} decay. Using the first forbidden unique shape correction factor and the modified response function, linear Fermi-Kurie plots were obtained with all detectors. Since consistent values of the endpoint energy were obtained with all of the detectors, the iteration procedure

was apparently independent of variations in counter resolutions up to 35 keV, the maximum resolution considered acceptable in a counter.

For the final value of the endpoint energy of the outer branch, five runs for the singles spectra using a 6 mm thick detector were made. Calibration spectra using the three sets of conversion lines in Bi^{207} were taken immediately before and after each run. If any drift was noted, the run was discarded. The source strength was kept sufficiently low so that no pileup beyond the maximum beta ray energy of the outer branch cound be observed. In both these and the coincidence runs, the solid state detector and the source were mounted near one wall of an aluminum vacuum chamber 45 cm in diameter and 15 cm high with a wall thickness of 5 mm. All of the solid state detectors were operated at room temperature in these experiments with bias voltages between 200 and 400 volts.

In the coincidence experiments, the output of the Tennelec 100A preamplifier used with the solid state detector was fed directly into both the multichannel analyzer and the distributed amplifiers preceding the fast coincidence circuit. The other channel of the coincidence circuit consisted of a 3" x 3" NaI(Tl) scintillation counter whose single channel pulse height analyzer was set to span the 1077 keV Rb^{86} gamma ray photopeak. With this arrangement, a resolving time of 60 ns was obtained with full efficiency down to beta ray energies of 200 keV. The real coincidence counting rate was maximized by placing the counters 180^{o} apart, with solid angle fractions of approximately 30% each. In addition, the source strength was kept sufficiently low so that the chance coincidence rate was less than 3% of the real coincidence rate. A total of five runs were taken with a 3 mm thick silicon detector, each run lasting 10 hours.

4. Results and conclusions

In the singles spectra taken on the outer branch, the outlined correction procedure was applied and a Fermi-Kurie plot constructed using the first forbidden unique shape correction factor. A typical plot is shown in fig. 5, which also shows a Fermi-Kurie plot of the spectrum uncorrected for the detector response function. The linearity of the corrected plot is quite good down to energies where beta rays from the inner branch occur. Fermi-Kurie plots of the coincidence spectra were made using no shape correction factor, and a typical plot is shown in fig. 6. No deviation from linearity within the limits of statistical error could be observed down to the electronic cutoff at 200 keV. This confirms previous results that the inner branch has an allowed shape.

The endpoint energies for the inner and outer branches determined from a simple analysis of this spectral data are 686 $\pm$ 20 keV and 1753.0 $\pm$ 4.5 keV. In order to obtain a better value for the energy of the inner branch, the previously determined gamma ray energy[11] was subtracted from the endpoint energy of the outer branch. This value was then combined with the coincidence results to give a final result of 677 $\pm$ 5 keV. Comparison with previous work is shown in table 1. In general, the values of the endpoint energies obtained in the current work are lower than other results, but are in close agreement with those of Macklin, Lidofsky and Wu.[5]

The authors wish to acknowledge the use of the Case Institute of Technology Univac 1107 Computer under a program sponsored in part by the National Science Foundation. They are also grateful to Mrs. H. M. Murray for her assistance in the fabrication of the silicon detectors. Finally, they are indebted to Mrs. M. Ratner for her assistance in preparing the computer programs.

Table 1

Peference	Endpoint energies (keV)	Shape
2)	716 ± 20 1822 ± 14	First-forbidden unique
3)	726 ± 10 1800 ± 10	First-forbidden unique
4)	680 ± 6 1770 ± 4	Allowed First forbidden unique
5)	670 ± 5 1760 ± 10	Allowed First-forbidden unique
6)	717 ± 14	
7)	700 ± 10 1820 ± 40	Allowed First-forbidden unique
Current work	676 ± 5 1753.0 ± 4.5	Allowed First-forbidden unique

References

1) E. B. Shera, K. J. Casper, and B. L. Robinson, Nuclear Inst. and Methods 24 (1963) 482

2) D. J. Zaffarano, B. D. Kern, and A. C. G. Mitchell, Phys. Rev. 74 (1948) 682

3) H. R. Muether and S. L. Ridgway, Phys. Rev. 80 (1950) 750

4) A. V. Pohm, W. E. Wewis, J. H. Talboy, Jr., and E. N. Jensen, Phys. Rev. 95 (1954) 1523

5) P. A. Macklin, L. J. Lidofsky and C. S. Wu, Phys. Rev. 82 (1951) 334A

6) R. L. Robinson and L. M. Langer, Phys. Rev. 112 (1958) 481

7) D. R. Cartwright, W. J. Paul, and J. D. Kurbatov, Bull. Am. Phys. Soc. No. 3 (1958) 206

8) H. M. Murray and K. J. Casper (to be published)

9) M. S. Freedman, T. B. Novey, F. T. Porter, and F. Wagner, Jr., Rev. Sci. Inst. 27 (1956) 716

10) R. T. Birge and J. W. Weinberg, Revs. Modern Phys 19 (1947) 298

11) J. W. Harpster, D. L. Bennett and K. J. Casper, Nuclear Phys. 47 (1963) 443

Figure captions

Fig. 1 Decay scheme of Rb^{86}.

Fig. 2 Typical spectrum of P^{32} measured with the solid state detector in the magnetic spectrometer. The spectrometer was set so that beta rays of 1200 keV energy were incident on the detector.

Fig. 3 Idealized response of the solid state detector to monoenergetic electrons. This simplified shape was assumed for all computer calculations.

Fig. 4 Plot of the relative number of counts measured correctly as a function of energy. In the idealized shape of fig 3, A_p corresponds to the area under the triangle, while A_T corresponds to the total area under both the triangle and the flat portion.

Fig. 5 Fermi-Kurie plot of the higher energy beta decay of Rb^{86}. Curve B is a plot with no correction made for the response function of the detector. Curve A is a plot with this response function taken into account. Both plots have been made using the first-forbidden unique shape correction factor.

Fig. 6 Fermi-Kurie plot of the inner branch using data from one of the coincidence runs. No shape correction factor has been applied.

Figure 1

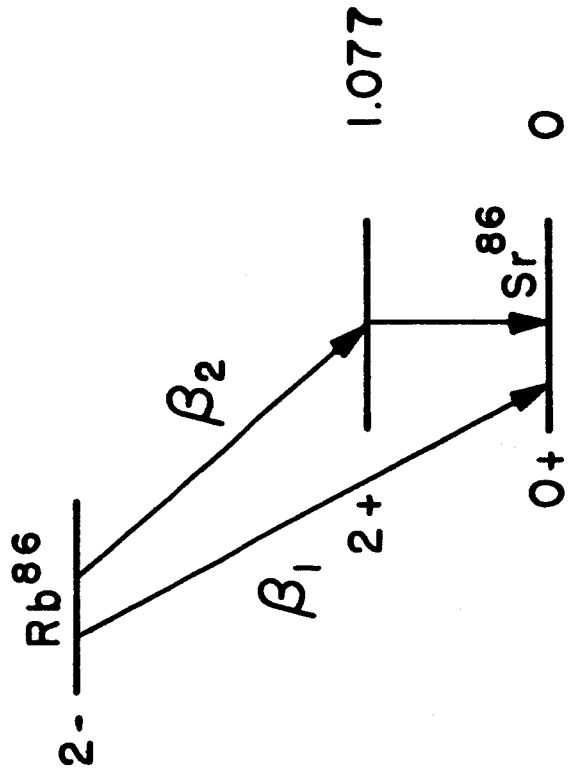

Figure 2

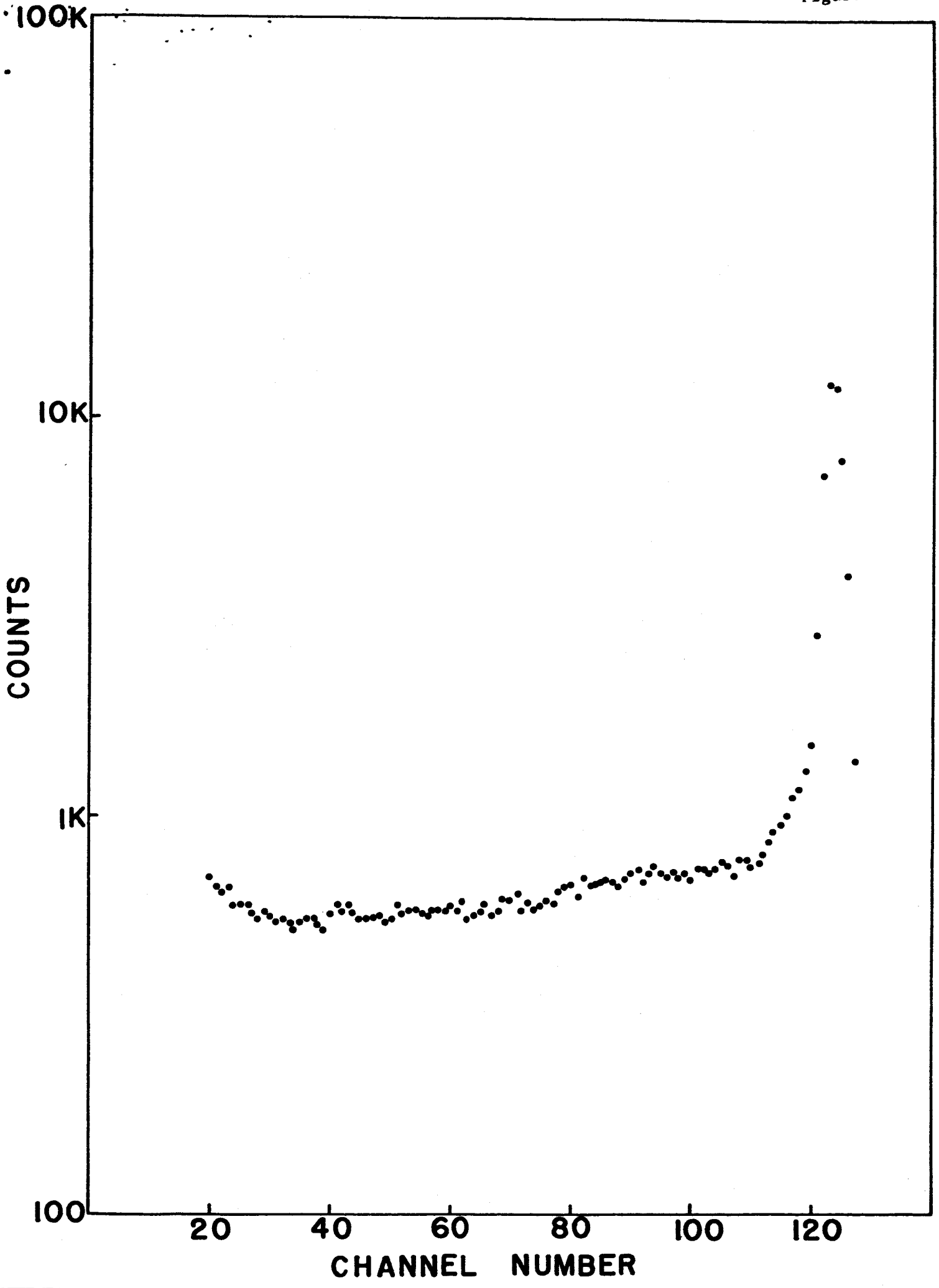

Figure 5

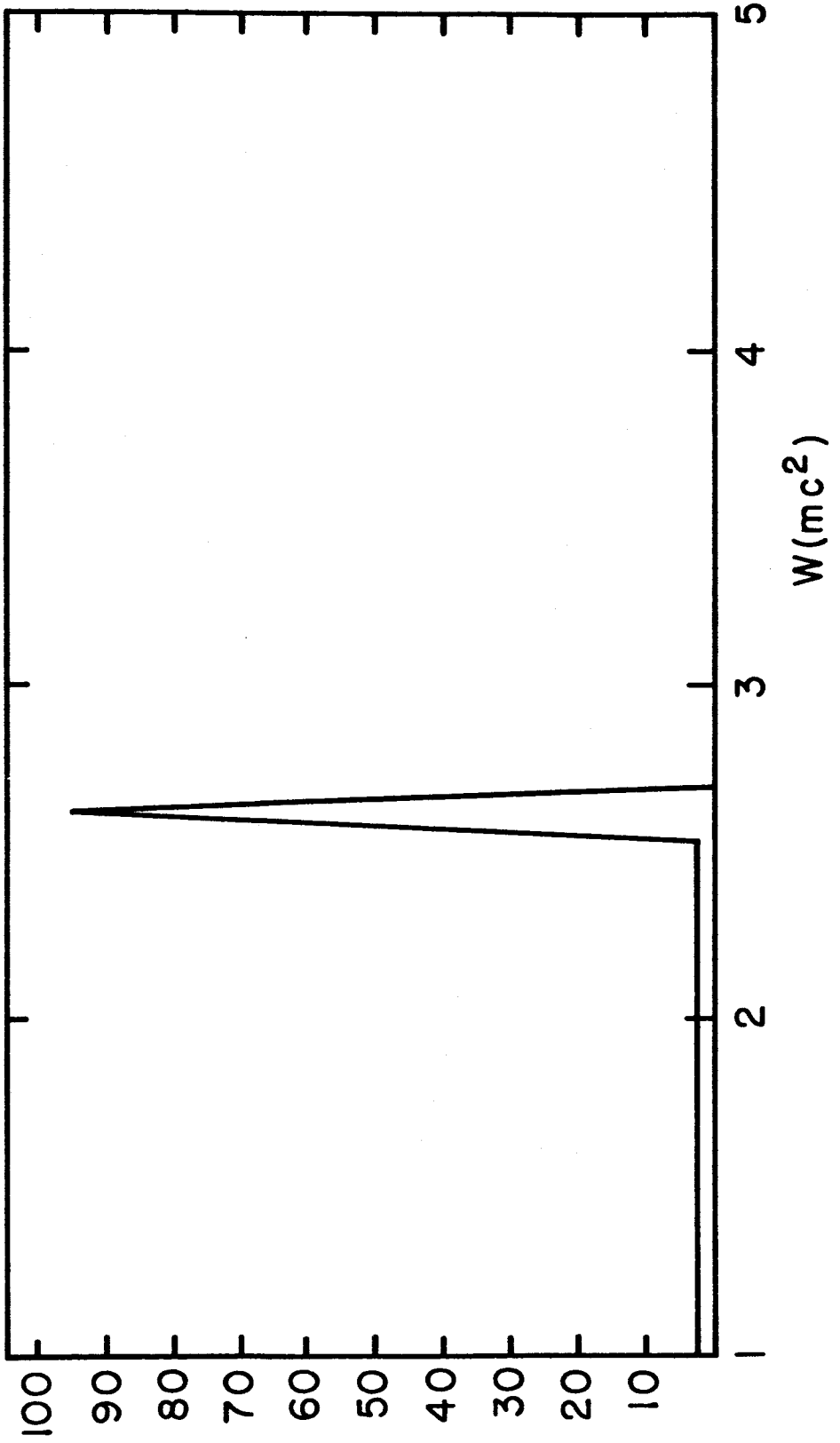

Figure .4

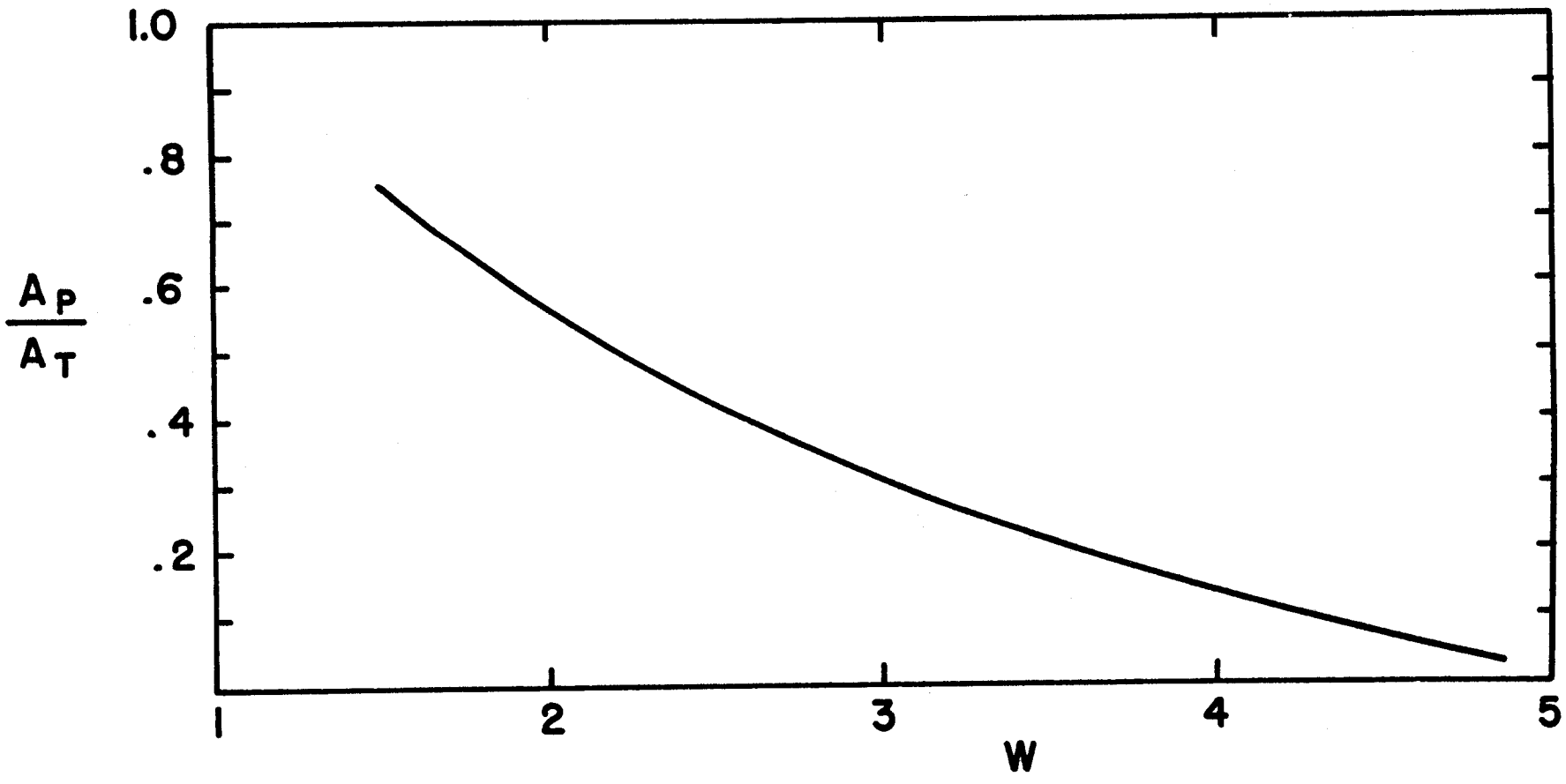

Figure 5

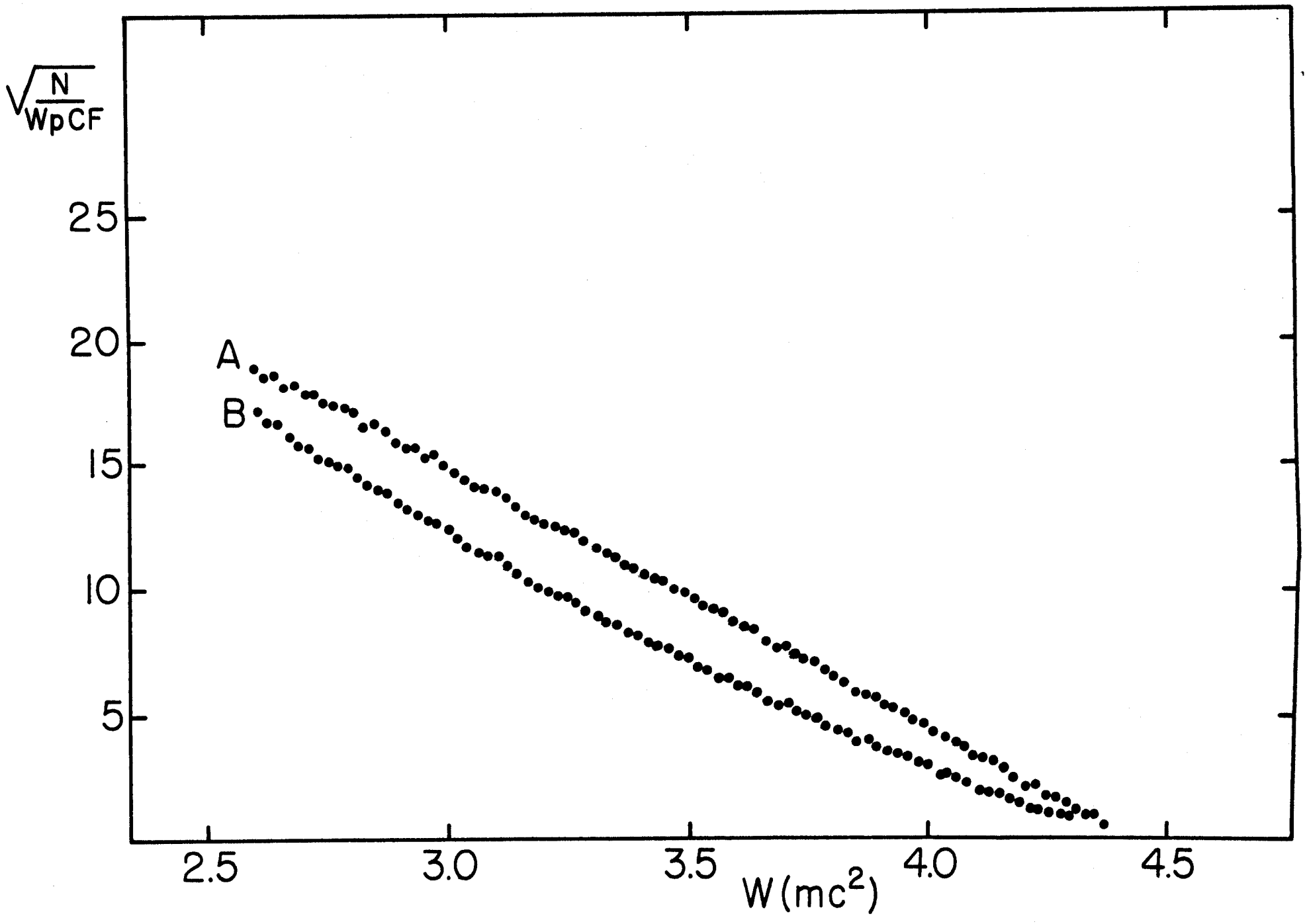

Figure 6